Environmental Engineering and Management Journal

May 2025, Vol. 24, No. 5, 1035-1041
http://www.eemj.icpm.tuiasi.ro/; http://www.eemj.eu
http://doi.org/10.30638/eemj.2025.079

"Gheorghe Asachi" Technical University of Iasi, Romania

ISOLATION, ANTIFUNGAL ACTIVITY, AND MOLECULAR DOCKING ANALYSIS OF AXILLARIN FROM *Tanacetum alyssifolium*

Samed Şimşek[1], Yusuf Bayar[2]*, Tuncay Karakurt[3], Hüseyin Akşit[4], Ekrem Köksal[5]

[1]Erzincan Binali Yıldırım University, Çayırlı Vocational School, Medical Services and Techniques Department, 20250, Erzincan, Turkey
[2]Department of Plant Protection, Faculty of Agriculture, Kırşehir Ahi Evran University, 40100, Kırşehir, Turkiye
[3]Department of Chemical Engineering, Faculty of Engineering and Architecture, Ahi Evran University, 40100, Kırşehir, Turkiye
[4]Erzincan Binali Yıldırım University, Faculty of Pharmacy, Department of Analytical Chemistry, 24100 Erzincan, Turkiye
[5]Erzincan Binali Yıldırım University, Faculty of Science and Art, Department of Chemistry, 24100 Erzincan, Turkiye

Abstract

The antifungal activity of axillarin, a polymethoxylated flavone isolated from the methanol extract of *Tanacetum alyssifolium*, was evaluated *in vitro* against several plant pathogenic fungi: *Fusarium oxysporum* f. sp. *radicis-lycopersici* (FORL), *Alternaria alternata* (A.A), *Fusarium oxysporum* f. sp. *niveum* (FON), *Phytophthora infestans*, and *Cylindrocarpon* spp. Antifungal efficacy was assessed at concentrations of 200 and 400 µg/mL using the agar Petri dish method. Axillarin inhibited fungal mycelial growth in a dose-dependent manner, with the highest inhibition observed for *A. alternata* (33.31%), followed by FORL (29.46%), *Cylindrocarpon* spp. (26.64%), and FON (18.21%). No inhibitory effect was detected against *P. infestans*.
To support the experimental findings, molecular modeling was performed using GaussView 5.0 and GAUSSIAN 09 to determine the optimized 3D conformation of axillarin through potential energy surface (PES) analysis. This optimized structure was then used in molecular docking simulations to explore interactions with fungal protein receptors.
The results suggest that axillarin may serve as a natural antifungal agent with potential applications in the development of environmentally friendly alternatives to synthetic fungicides. This approach supports sustainable plant protection strategies and reduces ecological risks associated with chemical pesticide use.

Key words: antifungal activity, axillarin, molecular docking, plant pathogens, *Tanacetum alyssifolium*

Received: May, 2023; Revised final: August, 2024; Accepted: October, 2024; Published in final edited form: May, 2025

1. Introduction

Fungi-derived infections are commonly controlled using synthetic chemical fungicides to protect agricultural crops and ensure food security. While effective, the widespread and long-term use of these chemical agents has raised serious concerns regarding environmental pollution, human health risks, and the development of resistant fungal strains. The ecological persistence of synthetic fungicides, their potential to contaminate soil and water, and their non-selective action on non-target organisms have intensified the demand for safer and more sustainable alternatives (Cushnie and Lamb, 2005; Guo and Tan, 2023). In response to these challenges, increasing attention has been directed toward natural sources of antifungal agents. Plant-derived extracts or isolated pure compounds, traditionally used in folk medicine and pest management, are now being investigated for their potent bioactive properties and environmental compatibility. Numerous antifungal compounds obtained from medicinal and aromatic plants have demonstrated promising efficacy against various phytopathogenic fungi, offering a biodegradable and less toxic option for integrated pest management strategies (Bajwa et al., 2008; Duke, 2002; Serrano et

* Author to whom all correspondence should be addressed: e-mail: yusuf.bayar@ahievran.edu.tr

al., 2005; Tripathi and Dubey, 2004). These natural products not only align with ecological safety goals but also support the transition toward environmentally friendly plant protection solutions.

Flavonoids are widely dispersed phenolic substances in all vascular plants. Numerous studies on flavonoids have shown that they have anti-inflammatory, antibacterial, antioxidant, and vascular benefits (Cushnie and Lamb, 2005; Galeotti et al., 2008). Furthermore, these compounds have a broad range of biological and pharmacological properties. Flavonoids were reported by many researchers to show antimicrobial activity (Baez et al., 1999; Di Carlo et al., 1999; Harborne and Williams, (1988).

The term 'polymethoxy flavone' is known to refer to compounds that have two or more methoxy groups. Due to the hydrophobicity of methoxy groups, polymethoxy flavones have more hydrophobic properties than those carrying hydroxyl groups. Therefore, polymethoxy flavones can reach much easily to the target cells (Walle, 2007). Many biological activities of polymethoxy flavones such as anti-inflammatory (Manthey et al., 2001), antioxidant (Anagnostopoulou et al., 2005), antiallergic (Kobayashi and Tanabe, 2006), anticancer (Ohnishi et al., 2004; Yoshimizu et al., 2004; Tang et al., 2007) have been studied.

Axillarin, a polymethoxylated flavone (5,7,3′,4′-tetrahydroxy-3,6-dimethoxy flavanol) is identified in various Asteraceae plants, including *Balsamorhiza macrophylla*, *Tanacetum vulgare*, *Pulicaria crispa*, *Filifolium sibiricum*, and *Inula britannica*. Previous studies on axillarin have reported antioxidant, anti-inflammatory effects, and probiotic properties (Hu et al., 2017; Turan et al., 2020).

In this study, we report the effects of the antifungal potency of axillarin isolated from *Tanacetum alyssifolium* against *Fusarium oxysporum* f. sp. *radicis-lycopersici* (FORL)*, Alternaria alternata* (A.A.), *Fusarium oxysporum* f. sp. *Niveum* (FON), *Phytophthora infestans,* and *Cylindrocarpon* spp. fungal pathogens. Another goal of the study is to evaluate the inhibition pattern of the 3V0R, 5A0E, 7BPC, and 5I7S receptors by axillarin using X-Ray crystal structures through molecular docking simulation.

2. Material and methods

2.1. Isolation of axillarin

The isolation and characterization of axillarin from *Tanacetum alyssifolium* was previously reported by our group (Köksal et al., 2020)**.** Briefly, the methanolic extract was fractionated over Sephadex LH-20 by eluting with methanol. Axillarin-containing fractions, identified by TLC, were combined and separated over a C18-packed column. The water and methanol mixture was used as follows: 10:0, 8:2, 7:3, and 6:4, each 0.5 L. Axillarin was obtained from the latter fraction. The solvents were evaporated to dryness and the obtained yellowish residue was dissolved in methanol and maintained at +4 ºC overnight to give a pale-yellow amorphous precipitate (Fig. 1).

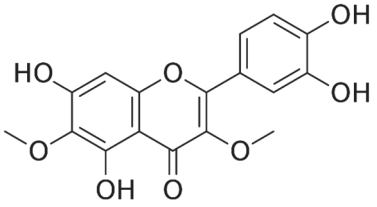

Fig. 1. Chemical structure of axillarin

2.2. Preparation of fungus cultures

The plant pathogen fungi used in this study were obtained from stock cultures found at Ahi Evran University, Faculty of Agriculture, Department of Plant Protection, Phytoclinical Laboratory. In these tests, young fungus cultures were used that developed for 7 days at 25±2 ºC in 90-mm Petri dishes containing 20-mL potato dextrose agar (PDA). The fungi used are shown in Table 1.

Table 1. List of plant pathogens

Plant pathogens	***Origin***
Fusarium oxysporum f.sp. *radicis-lycopersici* (FORL)	Tomato
Alternaria alternata	Apple
Fusarium oxysporum f. sp. *niveum*.	Watermelon
Phytophthora infestans	Potato
Cylindrocarpon sp.	Strawberry

2.3. In vitro antifungal activity

Potato dextrose agar (PDA) was prepared, autoclaved, and cooled to 40°C. Axillarin was mixed with sterile PDA to give final concentrations of 200 µg/mL and 400 µg/mL. PDA was transferred to 60 mm diameter Petri dishes (10 mL). Mycelium disks (5-mm diameter) obtained from 7 days old fungus cultures were transferred to Petri dishes. Fungus cultures were incubated at 25 ± 2°C for 7 days after inoculation. According to the control value growth inhibition percentage was calculated by comparing the growth of the mycelium development (Yilar et al., 2020). As a positive control, the standard fungicide Thiram 80% was used. The experiments were conducted with four replications and two parallels. Percent mycelium growth was calculated according to the following formula (Eq. 1).

$$I = 100 \times (dc-dt) / dc \quad (1)$$

where: I-Percent development of mycelium; dc-Development of mycelium in control; dt-Mycelium development behavior

2.4. Data analysis

The data were analyzed by analysis of variance using the SPSS 15 statistical package program and the differences between the means were determined by the

DUNCAN test. Differences were considered significant for $p<0.05$.

2.5. Computational study

A drug molecule with biological activity is assumed to have an active conformation among the existing low-energy conformations. Research into the most bioactive conformation among these conformation structures is one of the most important duties of medicinal chemistry. Specific molecules at the active site of receptor protein can only bind by interacting with bioactive conformation. Based on the knowledge about the active structure, novel agents can be designed for a particular receptor system. Describing low-energy conformations is a crucial step in understanding the relationship between a molecule's structure and its biological activity (Höltje et al., 2008). Theoretically, 2-dimensional potential energy surface (PES) scanning was performed via AM1(Dewar et al., 1985), a semi-empirical calculation method, by choosing θ (C13-C12-C1-C2) dihedral angle of the axillarin compound to identify the stable structure of the compound. The single point energy of each step was calculated by changing the chosen dihedral angle by 20˚ of angles within the range of +180˚/-180˚. Four conformations (conf1-4) (Fig. 1) of the molecule corresponding to the minimum energy were obtained because of PES analysis.

Conf 1 structure was determined to be the most stable one following the re-optimization procedures of these four conformations (Fig. 2). All the calculations were carried out on the conf1 that was the most stable structure.

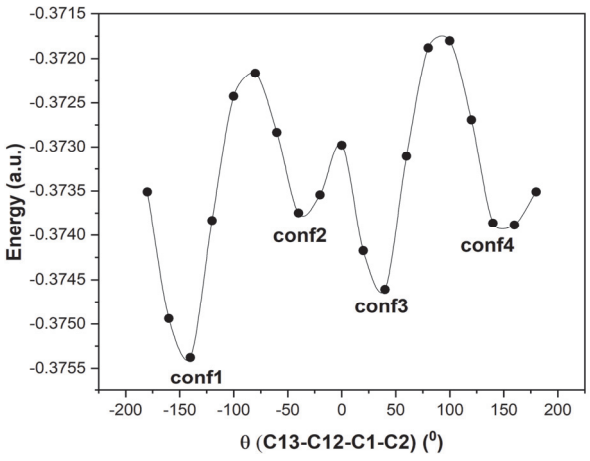

Fig. 2. Representation of Global and local minimums on the potential energy surface

2.6. Molecular docking simulations

Optimized structures of all compounds were designed via the Gaussian 09 (Frisch et al., 2009) program using the 6-311 G(d) (Becke, 1993) basis set and Density Functional Theory DFT/B3LYP (Lee et al., 1988; Becke, 1993). For molecular docking simulation procedures, PyRX (Dallakyan, 2008) program containing Autodock via (Trott and Olson, 2010) software with Lamarckian genetics as the scoring algorithm was used.

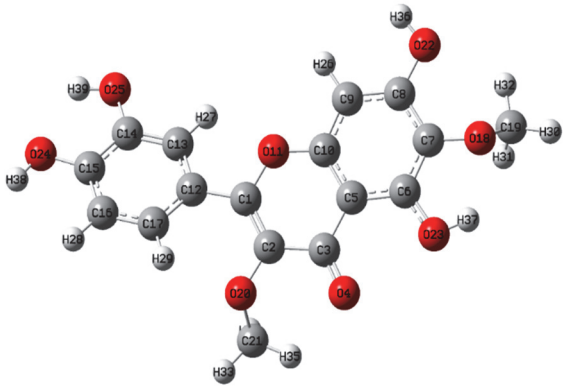

Fig. 3. The optimized conformation obtained by 2D PES analysis

2.7. Molecular electrostatic potentials (MEP)

The electron density surface of a molecule represents the maximum distance the electron density can reach The sites where the molecular electrostatic potential of a molecule is the most negative at the most refer to the site where the electrophilic attack is at the most. It provides important data about the formation of an intramolecular hydrogen bond. On the electrostatic potential map, while the most negative potential is indicated with red, blue is used to indicate the most positive potential (Cramer, 2003; Uzun et al., 2016; Zahradník and Polák, 1980). In the surface map of the molecule derived from the MEP map (Fig. 3), the orange represents the sites partly rich in negative charge or electrons and the yellow represents sites that partly have a deficiency of positive charge or electron.

As shown in Fig. 4, the most negative sites of the molecule are found around the atoms O4 and O23; whereas, the most positive sites are found around the hydrogen atoms bond to the atoms O24 and O22. Consequently, it can be asserted that these atoms in the compound will display a stronger interaction compared to other atoms in terms of ligand-receptor interaction.

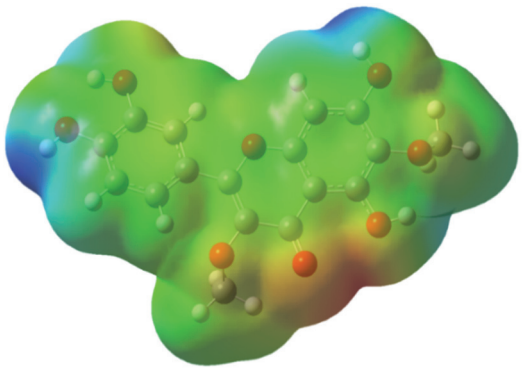

Fig. 4. Molecular electrostatic potential map of axillarin structure

3. Results and discussion

The *in vitro* antifungal activity of the axillarin compound against plant pathogenic fungi is presented in Table 2. The tests demonstrated varying degrees of inhibitory activity against the fungi. Plant pathogens' mycelium growth (MG) and mycelial growth inhibition (MGE) of axillarin are shown in Fig. 5 and Table 2. MG of plant pathogens was calculated in millimeters for *A. alternata*, FORL, *Cylindrocarpon* spp., FON, and *P. infestans* as 40.01, 44.01, 49.98, 54.33, and 60 mm, respectively.

Axillarin exhibited a dose-dependent inhibition of fungal mycelium growth. The most susceptible fungi to axillarin were 33.31% *A. alternata*, whereas FORL 26.64%, and *Cylindrocarpon* spp. 18.21% and FON followed with 29.46%. *P. infestance* did not affect the development of mycelium. Mycelium development of fungi of plant pathogens did not stop completely.

This study will be important for the human and environmental health of natural compounds to be developed against synthetic pesticides commonly used in the control of plant pathogens. Different medicinal aromatic plants contain various flavonoid fractions with antifungal properties. Propolis contains galangin, a flavonol shown to have antifungal activities against *Cladosporium sphaerospermum*, *Penicillium digitatum*, *A. tamarii*, *A. flavus,* and *P. italicum* (Cushnie and Lamb, 2005). The flavonoid-rich extracts obtained from *Sida acuta* showed antifungal activity against *Candida albicans* (Alka et al., 2012). In another study, eight flavonoids and five steroids isolated from *Chromolaena* species showed antimicrobial activity (Mishra and Verma, 2013).

3.1. Molecular docking studies

In molecular docking studies, X-ray crystal structures belonging to 3V0R (*Alternaria alternata* allergen Alt a 1: a unique beta-barrel protein dimer found exclusively in fungi) and 5I7S (Crystal structure of RXLR effector PexRD54 from *Phytophthora infestans*) were used. Figure 5 shows a 3-dimensional representation of receptor-ligand interactions and Fig. 6 shows 2-dimensional interactions between ligand and receptors. Receptors and axillarin compounds were prepared for docking procedures using protein and ligand preparation wizards included in the PyRx package. Tables 3-4 show affinity energy (docking scores) extracted by docking procedures. Fig. 6 displays a 3-dimensional view of the receptor-ligand interactions between axillarin ligand affiliated to active binding sites of target proteins and 3V0R with the highest docking score and 517S with the lowest score, and 2-dimensional interactions between ligand and receptors are shown in Fig. 7.

The axillarin ligand was observed to have classical hydrogen bond interactions with LEU107, ASP100, LEU106, GLY105, HIS84, and LYS85 residues in the active bonding sites of 3V0R receptor ALA103, ASN102, GLY72, GLN111, ARG82, and GLY75 residues in the active bonding sites of 5A0E receptor, ASN171, ARG170, MET143, and ILE176 residues in active bonding sites of 7BPC receptor, and ARG234 and ASP228 residues in active bonding sites of 5I7S receptor; whereas, the interactions between the 5I7S receptor and ligand were minimum.

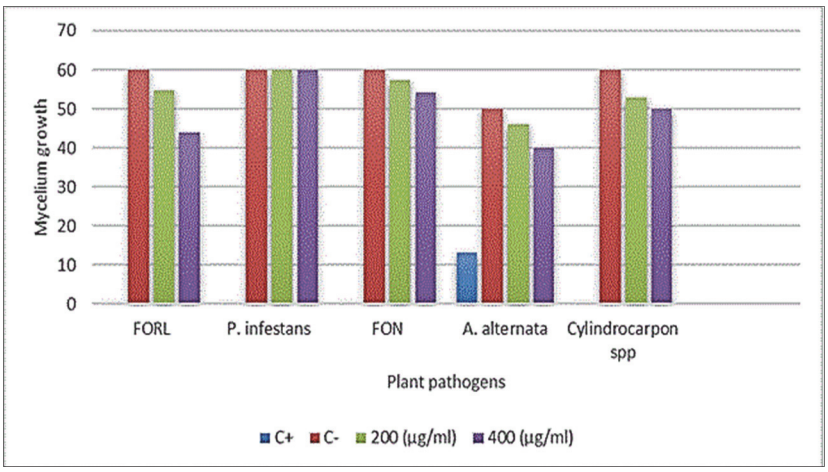

Fig 5. Effect of axillarin on mycelial growth of FORL; *Fusarium oxysporum* f.sp. *radicis-lycopersici,* FON; *Fusarium oxysporum* f. sp. *niveum*, *Cylindrocarpon* spp., *A.alternata* and *P. İnfestans*

Table 2. The effect of axillarin on the % mycelial growth inhibition of plant pathogenic fungi

Doses (µg/mL)	*FORL*	*FON*	*A. alternata*	*Cylindrocarpon spp.*	*P. infestans*
C^-	0.00±0.00d	0.00±0.00d	16.70±0.00d	0.00±0.00d	0.00±0.00b
200	8.93±0.74 c	4.32±0.89c	23.01±1.86 c	11.93±0.75c	0.00±0.00b
400	26.64±1.68 b	9.46±0.45b	33.31±1.83 b	18.21±0.48 b	0.00±0.00b
C^+	100±0.00 a*	100±0.00a	77.73±0.00 a	100±0.00 a	100±0.00 a

*Differences were considered significant for $p<0.05$. C+=Positive Control (Thiram 80%), C-= Negative Control (Aceton 10%), FORL; *Fusarium oxysporum* f.sp. *radicis-lycopersici,* FON; *Fusarium oxysporum* f. sp. *niveum*

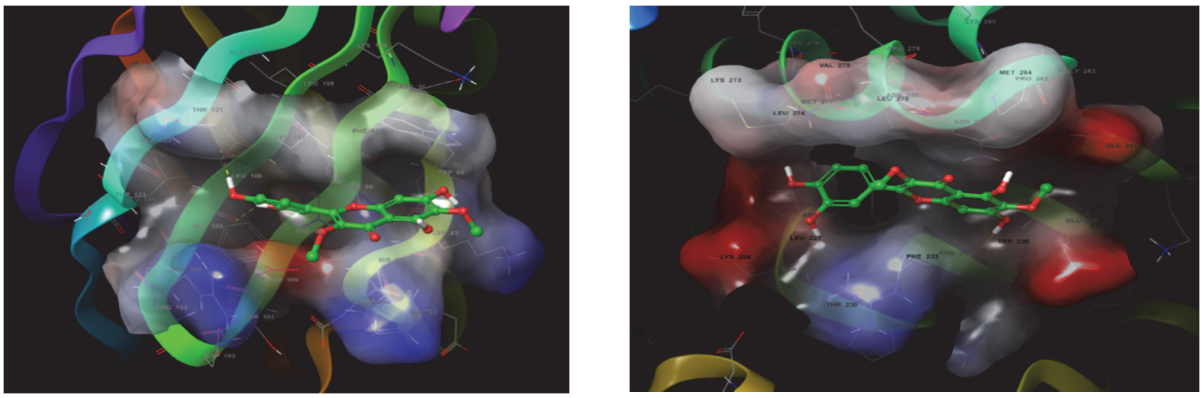

(a) (b)

Fig. 6. 3D Interactions between: (a) 3V0R, (b) 5I7S receptors and axillarin

Additionally, all ligands were seen to bind with alkyl and hydrophobic interactions as well. Axillarin interacts with the 3V0R receptor through 5 hydrogen bonds and hydrophobic interactions at distances of 3.88 and 3.84 Å. The docking score obtained for this interaction is 6.9 kcal/mol. Hydrogen bonds represent strong electrostatic interactions between the ligand and the receptor. The presence of 5 hydrogen bonds indicates a high-affinity and specific binding of axillarin to 3V0R, with these bonds being formed at specific conformations in the binding site. Hydrophobic interactions, occurring at distances of 3.88 and 3.84 Å, contribute to the stabilization of the complex by facilitating interactions between hydrophobic regions and excluding water molecules. The strength of these interactions contributes to the high docking score.

For the 5I7S receptor, axillarin forms 4 hydrogen bonds and hydrophobic interactions at distances of 5.16 and 5.02 Å. The resulting docking score is 6.5 kcal/mol. The presence of 4 hydrogen bonds indicates a strong binding affinity, though slightly less than with 3V0R. The longer hydrophobic interaction distances (5.16 and 5.02 Å) suggest that these interactions might be less effective or involve different conformational dynamics compared to those observed with 3V0R. These factors contribute to the slightly lower docking score observed for 5I7S.

These data show that axillarin forms strong and specific interactions with both receptors. Besides the docking scores, the number and distances of hydrogen bonds and hydrophobic interactions provide significant insights into the binding mechanisms of axillarin. Hydrogen bonds contribute to stabilization through electrostatic attraction in the binding region, while hydrophobic interactions help stabilize the complex by interacting hydrophobic pockets. Understanding these molecular interactions enhances our understanding of axillarin's biological effects and potential therapeutic applications.

According to Fig. 5, the ligand had a better settlement in the gap site within the binding site of the 7BPC receptor. As a result, the binding affinity of the axillarin ligand with 3V0R was higher than that of the 5I7S receptor. It is seen that the results of our molecular docking studies and in-vitro studies are parallel to each other. In-vitro studies, it was supported by the molecular docking result that the axillarin molecule was more effective on *A. alternata*.

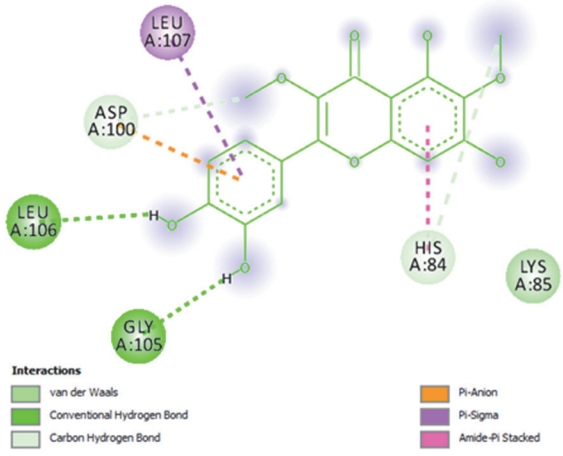

(a)

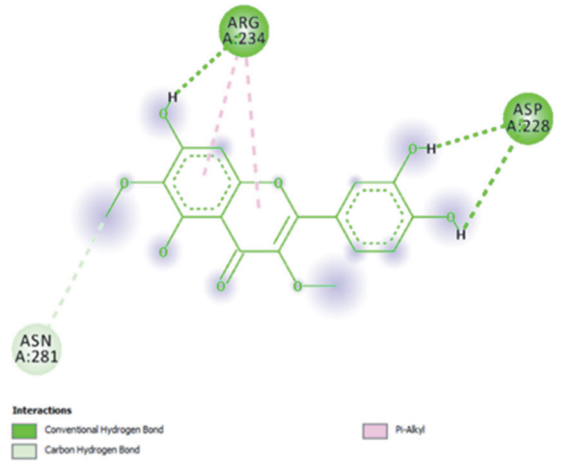

(b)

Fig. 7. 2D Interactions between a) 3V0R b) 5I7S receptors and molecule axillarin

Table 3. Interactions between axillarin and 3V0R receptor

Name	*Affinity (kcal/mol)*	*Distance donor/ acceptor*	*Interaction category*	*Interaction types*	*Donor group*	*Donor group types*	*Acceptor group*	*Acceptor group Types*
d:***0:H - A:GLY105:O	-6.9	1.95025	Hydrogen bond	Conventional hydrogen bond	d:***0:H	H-donor	A:GLY105:O	H-acceptor
d:***0:H - A:LEU106:O		2.54469	Hydrogen bond	Conventional hydrogen bond	d:***0:H	H-donor	A:LEU106:O	H-acceptor
d:***0:H - d:***0:O		2.29152	Hydrogen bond	Conventional hydrogen bond	d:***0:H	H-donor	d:***0:O	H-acceptor
d:***0:C - A:ASP100:OD2		3.61579	Hydrogen bond	Carbon hydrogen bond	d:***0:C	H-donor	A:ASP100:OD2	H-acceptor
d:***0:C - A:HIS84:O		3.60652	Hydrogen bond	Carbon hydrogen bond	d:***0:C	H-donor	A:HIS84:O	H-acceptor
A:ASP100:OD2 - d:***0		3.57368	Electrostatic	Pi-anion	A:ASP100:OD2	Negative	d:***0	Pi-orbitals
A:LEU107:CD2 - d:***0		3.88288	Hydrophobic	Pi-sigma	A:LEU107:CD2	C-H	d:***0	Pi-orbitals
A:HIS84:C,O;LYS85:N - d:***0		3.84544	Hydrophobic	Amide-Pi stacked	A:HIS84:C,O; LYS85:N	Amide	d:***0	Pi-orbitals

Table 4. Interactions between ligand axillarin and 5I7S receptor

Name	*Affinity (kcal/mol)*	*Distance donor/ acceptor*	*Interaction category*	*Interaction types*	*Donor group*	*Donor group types*	*Acceptor group*	*Acceptor group types*
d:***0:H - A:ASP228:O	-6.5	2.59514	Hydrogen bond	Conventional hydrogen bond	d:***0:H	H-donor	A:ASP228:O	H-acceptor
d:***0:H - A:ASP228:OD2		2.9445	Hydrogen bond	Conventional hydrogen bond	d:***0:H	H-donor	A:ASP228:OD2	H-acceptor
d:***0:H - A:ARG234:O		1.81756	Hydrogen bond	Conventional hydrogen bond	d:***0:H	H-donor	A:ARG234:O	H-acceptor
d:***0:C - A:ASN281:OD1		3.72252	Hydrogen bond	Carbon hydrogen bond	d:***0:C	H-donor	A:ASN281:OD1	H-acceptor
d:***0 - A:ARG234		5.16143	Hydrophobic	Pi-Alkyl	d:***0	Pi-orbitals	A:ARG234	Alkyl
d:***0 - A:ARG234		5.02215	Hydrophobic	Pi-Alkyl	d:***0	Pi-orbitals	A:ARG234	Alkyl

4. Conclusions

This study demonstrated the antifungal potential of axillarin, a polymethoxylated flavone isolated from *Tanacetum alyssifolium*, through both *in vitro* experiments and molecular docking simulations. Axillarin exhibited dose-dependent inhibitory effects on the mycelial growth of several phytopathogenic fungi, with the highest inhibition observed against *Alternaria alternata*, followed by *Fusarium oxysporum* f. sp. *radicis-lycopersici* and *Cylindrocarpon* spp. Notably, no inhibitory effect was observed against *Phytophthora infestans*, indicating selective antifungal activity.

Computational studies provided additional insight into the mode of action of axillarin. Molecular docking simulations revealed strong binding affinity of axillarin toward the 3V0R receptor, with multiple hydrogen bonds and hydrophobic interactions contributing to its stabilization. The interaction profile supported the *in vitro* findings, particularly the higher susceptibility of *A. alternata*, which is associated with the 3V0R receptor. Molecular electrostatic potential analysis further identified key active sites (O4, O23, O22, and O24) as critical for ligand-receptor binding, suggesting structural regions of axillarin important for its antifungal activity.

These findings support the potential of axillarin as a natural antifungal compound with specific molecular targets. The combination of experimental and computational approaches strengthens the understanding of its bioactivity and paves the way for further structure-activity relationship studies and the design of new antifungal agents derived from natural products. Future work may focus on the synthesis of axillarin analogs, *in vivo* assessments, and formulation development for agricultural or pharmaceutical applications.

5. References

Alka J., Padma K., Chitra J., (2012), Antifungal activity of flavonoids of *Sida acuta* Burm f. against *Candida albicans, International Journal of Drug Development and Research*, **4**, 92-96.

Anagnostopoulou M.A., Kefalas P., Kokkalou E., Assimopoulou A.N., Papageorgiou V.P., (2005), Analysis of antioxidant compounds in sweet orange peel by HPLC–diode array detection–electrospray ionization mass spectrometry, *Biomedcal Chromatogr*, **19**, 138-148.

Baez D.A., Zepeda Vallejo L.G., Jimenez-Estrada M., (1999), Phytochemical studies on *Senna skinneri* and *Senna wislizeni*, *Natural Product Letters*, **13**, 223-228.

Bajwa R., Javaid A., Shafique S., Javaid A., Jabeen K., Shafique S., (2008), Fungistatic activity of aqueous and organic solvent extracts of rice varieties on phytophathogenic fungi, *Allelopathy Journal*, **22**, 363-70.

Becke D.A., (1993), Density-functional thermochemistry. III. The role of exact exchange, *The Journal of Chemical Physics*, **98**, 5648, https://doi.org/10.1063/1.464913.

Cramer C.J., Bickelhaupt F., (2003), Essentials of computational chemistry, *Angewandte Chemie*, **42**, 381-391.

Cushnie T.T, Lamb A.J., (2005), Antimicrobial activity of flavonoids*, International Journal of Antimicrobial Agents*, **26**, 343-56.

Dallakyan S., (2008), *PyRx-python prescription v. 0.8. The Scripps Research Institute*, On line at: https://pyrx.sourceforge.io/

Dewar M.J., Zoebisch E.G., Healy E.F., Stewart J.J., (1985), Development and use of quantum mechanical molecular models. 76. AM1: a new general purpose quantum mechanical molecular model, *Journal of the American Chemical Society*, **107**, 3902-3909.

Di Carlo., G, Mascolo., N, Izzo., A.A., (1999), Capasso, F. Flavonoids: old and new aspects of a class of natural therapeutic drugs, *Life Sciences*, **65**, 337-353.

Duke J.A., (2002), *Handbook of Medicinal Herbs*, 1st Edition, CRC Press, Boca Raton, Florida, United States.

Frisch M., Trucks G., Schlegel H., Scuseria G., Robb M., Cheeseman J., (2009), *Gaussian 09, revision d.01*, Gaussian Inc., Wallingford CT, USA.

Galeotti F., Barile E., Curir P., Dolci M., Lanzotti V., (2008), Flavonoids from carnation (*Dianthus caryophyllus*) and their antifungal activity, *Phytochemistry Letters*, **1**, 44-48.

Guo J., Tan L., (2023), Safety assessment and provincial-scale spatial variation of pesticide use in China, *Environmental Engineering and Management Journal*, **22**, 1621-1632.

Höltje H.-D., Sippl W., Rognan D., Folkers G., (2008), *Molecular Modeling, Basic Principles and Applications*, 3rd Edition, Wiley-VCH, Weinheim, Germany.

Hu J., Ma W., Li N., Wang K.J., (2017), Antioxidant and anti-inflammatory flavonoids from the flowers of Chuju, a medical cultivar of *Chrysanthemum morifolim* Ramat, *Journal of the Mexican Chemical Society*, **61**, 282-289.

Kobayashi S., Tanabe S., (2006), Evaluation of the anti-allergic activity of *Citrus unshiu* using rat basophilic leukemia RBL-2H3 cells as well as basophils of patients with seasonal allergic rhinitis to pollen**,** *International Journal of Molecular Medicine*, **17**, 511-515.

Köksal E., Ulutaş Y., Şimşek S., Bayraktar T., Altay A., Çatır M., (2020), Isolation, characterization and antiproliferative activity of secondary metabolites from *Tanacetum alyssifolium* (Bornm.) Grierson, *Records of Natural Products*, **15**, 122-129.

Lee C., Yang W., Parr R.G., (1988), Development of the Colle-Salvetti correlation-energy formula into a functional of the electron density, *Physical Review B*, **37**, 785, https://doi.org/10.1103/PhysRevB.37.785

Manthey J.A., Guthrie N., Grohmann K., (2001), Biological properties of citrus flavonoids pertaining to cancer and inflammation, *Current Medicinal Chemistry*, **8**, 135-53.

Mishra R., Verma D.L., (2013), Antifungal activity of *Cheilanthes grisea* Blanford*. International Journal of Research and Development in Pharmacy & Life Sciences,* **2**, 333-6.

Ohnishi H., Asamoto M., Tujimura K., Hokaiwado N., Takahashi S., Ogawa K., (2004), Inhibition of cell proliferation by nobiletin, a dietary phytochemical, associated with apoptosis and characteristic gene expression, but lack of effect on early rat hepatocarcinogenesis in vivo, *Cancer Science*, **95**, 936-942.

Serrano M., Martinez-Romero D., Castillo S., Guillén F., Valero D., (2005), The use of natural antifungal compounds improves the beneficial effect of MAP in sweet cherry storage, *Innovative Food Science and Emerging Technologies*, **6**, 115-123.

Tang M., Ogawa K., Asamoto M., Hokaiwado N., Seeni A., Suzuki S., (2007), Protective effects of citrus nobiletin and auraptene in transgenic rats developing adenocarcinoma of the prostate (TRAP) and human prostate carcinoma cells, *Cancer Science*, **98**, 471-477.

Tripathi P., Dubey N.K., (2004), Exploitation of natural products as an alternative strategy to control postharvest fungal rotting of fruit and vegetables, *Postharvest Biology and Technology*, **32**, 235-245.

Trott O., Olson A.J., (2010), AutoDock Vina: improving the speed and accuracy of docking with a new scoring function, efficient optimization, and multithreading, *Journal of Computational Chemistry*, **31**, 455-461.

Turan N.Ü., Çelebioğlu H.U., Akşit H., Recep T., (2020), Insight into effects of Axillarin and Verbascoside isolated from *Tanacetum alyssifolium* and *Plantago euphratica* on probiotic properties of *Lactobacillus acidophilus* and *Lactobacillus rhamnosus*, *Biotech Studies*, **29**, 47-54.

Uzun S., Koşar B., Esen Z., Koç E., (2016) A Density functional study for nonlinear optical properties of a biologically active Quinoline derivative in different media*. Afyon Kocatepe Üniversitesi Uluslararası Mühendislik Teknolojileri ve Uygulamalı BilimLer Dergisi*, **16**, 59-66.

Walle T., (2007), Methoxylated flavones, a superior cancer chemopreventive flavonoid subclass?, *Seminars in Cancer Biology*, **17**, 354-362.

Harborne J.B., Williams C.A., (1988), *Flavone and Flavonol Glycosides,* In: *The Flavonoids: Advances in Research Since*, Harborne J. (Ed.), Boca Raton, Florida, United States: CRC Press, 303-328.

Yilar M., Bayar Y., Bayar A.A.A., Genc N., (2020), Chemical composition of the essential oil of *Salvia bracteata* Banks and the biological activity of its extracts: antioxidant, total phenolic, total flavonoid, antifungal and allelopathic effects, *Botanica Serbica,* **44**, 71-79.

Yoshimizu N., Otani Y., Saikawa Y., Kubota T., Yoshida M., Furukawa T., (2004), Anti-tumour effects of nobiletin, a citrus flavonoid, on gastric cancer include: antiproliferative effects, induction of apoptosis and cell cycle deregulation, *Alimentary Pharmacology & Therapeutics*, **20**, 95-101.

Zahradník R., Polák R., (1980), *Elements of Quantum Chemistry*, Springer, New York, USA.